*Article*

# Analysis of the Influence of Energy Group Structure on Iron Shielding Calculation

Jun Wu [ORCID], Bin Zhang * and Yixue Chen

School of Nuclear Science and Engineering, North China Electric Power University, Beijing 102206, China
* Correspondence: zhangbin@ncepu.edu.cn

**Abstract:** The energy group structure of a multi-group cross section library matched with a deterministic method has a significant influence on shielding calculation. The complex resonance cross section of Fe-56 has a significant influence on accuracy with different energy group structures when processing multi-group cross section data. In this study, in order to more accurately test the influence of the iron resonance phenomenon on shielding calculations, this group structure is modified by the 199-group with 69 points interpolated into its group boundaries at an energy range from 1.1 keV to 3.1164 MeV. The new 269-group library is then tested with selected SINBAD iron sphere benchmarks and compared with the results of 199-group, 299-group, and 172-group libraries and measurements. Upon analysis, it is shown that the resonance of Fe-56 has a great influence on the accuracy of the calculated leakage. Further, it is noted that the finer the energy group division, the greater the calculated leakage fluctuation, and the deeper the neutron passes through the iron sphere, the larger the calculated leakage fluctuation. This study and its leakage results may provide a good reference for the development of new multi-group structures for present and future shielding design.

**Keywords:** discrete ordinate method; multi-group structure; iron shielding benchmarks; resonance

## 1. Introduction

The energy group structure of a multi-group cross section library matched with a deterministic method, e.g., the discrete ordinate method ($S_N$) [1], has a significant influence on shielding calculation. When the number of energy groups is small, the calculation time is less, but the accuracy may not meet the specified requirements. Finer energy group numbers perform better in accuracy but require more calculation time. Thus, it is necessary to find a balance between these two factors when selecting an energy group structure.

In the 1950s, because the proliferation theory was not applicable to the calculation of small nuclear devices, the Los Alamos National Laboratory (LANL) of the United States developed a code based on the $S_N$ method. In order to provide basic cross section data for calculation, LANL successively used the Hansen–Roach 6-group library and Hansen–Roach 16-group library without resonance processing [2]. With the development of nuclear technology, some large fast reactor and thermal reactor projects were researched and designed, and the generation and research of multi-group cross section libraries were biased towards reactor core designs. At this time, the resonance processing of the unresolved resonance energy region of U-235, U-238, and other nuclides was very important. The former Soviet Union developed the Bondarenko 26-group library and the Bondarenko method [3], which is still widely used in the generation of multi-group libraries. The method of generating multi-group libraries for reactor core calculation was also developing towards refining the energy group structure. For example, Santamarina, A. et al. developed the SHEM multi-group libraries supporting the commercial program APOLLO with 281, 361, and other different energy group structures [4]. The commercial code CASMO5 [5] had 586 groups of the matched multi-group library. The classical WIMS 69-group and WIMS 172-group libraries [6] updated by the International Atomic Energy Agency (IAEA)

were also for reactor design. Although refining the energy group structure can make the influence of the weight function negligible when generating libraries, this treatment has great limitations with respect to the shielding calculation of the $S_N$ method, especially in considering the up-scattering effect, which greatly affects the calculation speed.

With the development of shielding design requirements, the generation of shielding multi-group cross section libraries has gradually attracted more attention. The Oak Ridge National Laboratory (ORNL) of the United States continued to research and develop the VITAMIN-B and BUGLE series multi-group cross section libraries for light water reactor shielding design for many years [7]. BUGLE is obtained by VITAMIN according to the neutron flux in various areas of a light water reactor as a weight function, which is only applicable to calculation for pressurized water reactors. The VITAMIN and BUGLE libraries are now widely used. The latest VITAMIN-B7 and BUGLE-B7 are also applicable to the shielding calculation of LWR, but they are not significantly improved compared with VITAMIN-B6 and BUGLE-96 [8]. Alpan, F. A. et al. developed the contribution and continuous point cross section driving method (CPXSD) for making fine energy groups and wide groups [9]. Although the weight function is optimized by combining the continuous point cross section to study the importance and contribution of energy groups of key nuclides, this method still requires the users to have rich experience in shielding calculation to analyze the relevant characteristics of key nuclides.

The focus material iron is an important shielding material which should be considered in shielding design. The complex resonance cross section of Fe-56 has a significant influence on accuracy with different energy group structures when processing multi-group cross section data. The neutron-induced reaction cross sections of Fe-56 have been reevaluated and improved in recently released evaluated nuclear data libraries. For example, JENDL5.0 was released in December, 2021 [10], ENDF/B-8.0 was released in February, 2018 [11], and CENDL-3.2 was released in June, 2020 [12]. Thus, further analysis is needed with respect to energy group structures.

In this study, the 199-group structure is refined according to the resonance peak of the total cross section of Fe-56; thus, the 269-group is formed. Four group structures—269-group, 199-group, 299-group, and 172-group—are tested and examined by performing shielding calculations for selected SINBAD [13] benchmark problems. Section 2 briefly explains multi-group cross section data matched with the $S_N$ method and how to generate multi-group cross section libraries from the Evaluated Nuclear Data Library. Section 3 describes the configuration of the selected SINBAD problems for shielding analysis. Section 4 presents the results of the selected SINBAD shielding analyses calculated using the deterministic method with the four energy group structures. A summary and conclusions are given in Section 5.

## 2. Multi-Group Libraries

### 2.1. Multi-Group for $S_N$ Method

Multi-group cross sections are normally used by computer codes of the deterministic method. The distributions of neutrons or photons in space and energy can be calculated with the method. It can also compute the results of criticality, leakage, or dose to personnel. The multi-group neutral particle transport equation expanded using Legendre polynomials in each energy group $g$ is:

$$\mu \frac{\partial}{\partial x} \phi_g(x, \mu) + \sum_{l=0}^{\infty} P_l(\mu) \sigma_{tlg}(x) \phi_{lg}(x)$$
$$= \sum_{l=0}^{\infty} \frac{2l+1}{2} P_l(\mu) \sum_{g'} \sigma_{Xlg' \to g}(x) \phi_{lg'}(x) + Q_g(x, \mu) \tag{1}$$

where the flux $\phi_g$ is allowed to vary with direction with polar cosine $\mu$ and position $x$. The Legendre expanded flux $\phi_{lg}$ and macroscopic total cross section $\sigma_{tlg}$ only vary with position. The Legendre expanded transfer cross section $\sigma_{Xlg' \to g}$ ($X$ includes the scattering cross section $\sigma_s$ and fission cross section $\sigma_f$) also varies with position. Because it is normally

assumed to depend only on $\mu$, $Q_g$ is a fixed or external source. The multi-group cross sections can be obtained from the equations below:

$$\sigma_{tlg}(x) = \frac{\int_g \sigma_t(x, E)\phi_l(x, E)dE}{\int_g \phi_l(x, E)dE},$$
(2)

and

$$\sigma_{Xlg' \to g} = \frac{\int_g dE \int_g dE' \sigma_{Xl}(x, E' \to E)\phi_l(x, E)}{\int_g \phi_l(x, E)dE}.$$
(3)

In this study, the discrete ordinate method ($S_N$) was used to analyze the neutron leakage from the devices which was compared with the measurement value. In this case, the multi-group cross section should match the $S_N$ method. The $S_N$ neutron transport equation is

$$\mu \frac{\partial}{\partial x}\phi_g(x, \mu) + \sigma_g^{S_N}\phi_g(x, \mu)$$
$$= \sum_{l=0}^{N} \frac{2l+1}{2} P_l(\mu) \sum_{g'} \sigma_{slg' \to g}^{S_N}(x)\phi_{lg'}(x) + S_{fg} + Q_g(x, \mu),$$
(4)

By comparing Equation (4) with (1), it is observed that the $S_N$ equations require cross sections as:

$$\sigma_{slg' \to g}^{S_N} = \sigma_{slg' \to g}, \ g' \neq g,$$
(5)

and

$$\sigma_{slg \to g}^{S_N} = \sigma_{slg \to g} - \sigma_{tlg} + \sigma_g^{S_N},$$
(6)

where $\sigma_g^{SN}$ is determined as an extended transport approximation:

$$\sigma_g^{S_N} = \sigma_{t,N+1,g} - \sum_{g'} \sigma_{slg \to g'}.$$
(7)

Strong anisotropic scattering often occurs at the reaction of induced neutrons with high energy that have collided with the light- or medium-mass nuclei of shielding materials. This transport approximation could correct for anisotropy in the scattering matrix and is especially effective for forward-peaked scattering.

In order to eliminate the deviation introduced by the approximate treatment of geometric structures, benchmarks with simple geometry and composition are usually used in the testing and analysis of multi-group cross section data. Thus, in this study, the code ARES [14] developed by North China Electric Power University (NCEPU) was employed. Its one-dimensional $S_N$ calculation module has the same function as code ANISN [15] and the matching macro cross section processing code TRANSX [16]. In this study, the parameters $P_7$ and $S_{16}$ were set to perform the leakage spectrum calculations of iron shielding benchmarks.

## 2.2. Generating Multi-Group Libraries

Resonance has a great influence on the processing flow of transport approximation. A rebalancing method was employed to attempt solving this problem by recalculating the effective resonance integral of the total and absorption cross sections after transport approximation. However, if the energy group structure does not match the resonance of the important nuclides, the reaction cross section may still have a large deviation after rebalancing. In this study, it was noted that the neutron-induced elastic and capture cross section of Fe-56 had a significant influence on iron shielding calculation. Fe-56 is the most important isotope of shielding materials, and its cross section has very significant resonance in the energy range of 10.0 keV to 1.0 MeV (basically contributed by elastic scattering), as shown in Figure 1.
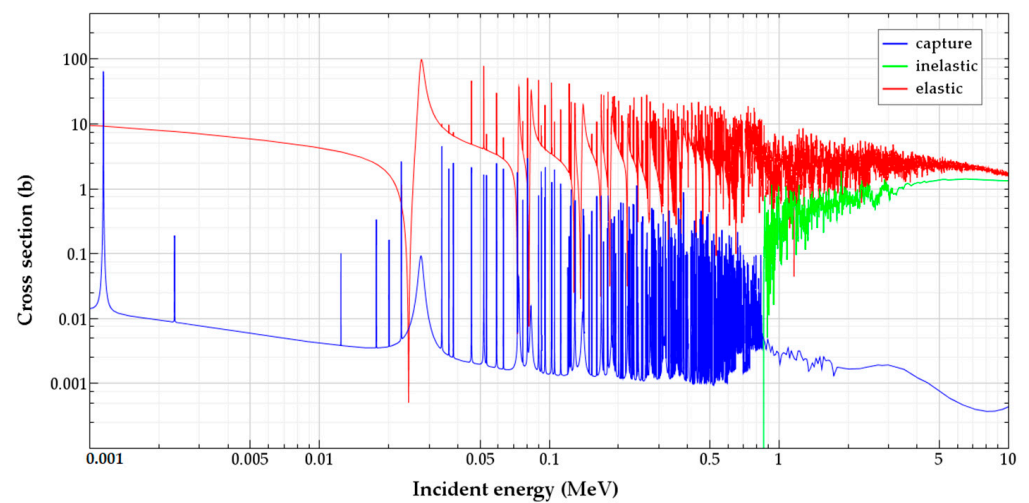
**Figure 1.** Radiation capture cross section (blue line), inelastic cross section (green line), and elastic cross section (red line) of Fe-56 in energy range of 1.0 keV to 10.0 MeV (CENDL-3.2).

The weight function and energy group structure simultaneously affect the accuracy of the generated multi-group cross sections. The weight functions of different devices or different regions of devices may lead to unexpected results. This should be considered when developing a multi-group cross section library. However, with the finer division of the energy group, the influence of the weight function on the results is smaller. The standard spectrum (Maxwell + 1/E + fission) was selected in this study; because the energy group structure was divided to a sufficiently fine degree, the influence of different weight functions on the calculation accuracy could be ignored. Our only focus was, therefore, whether the energy group structure was appropriate and especially whether it matched the resonance peaks of Fe-56.

When developing a multi-group library, the division of the energy group structure should follow this principle. One important resonance peak of the important nuclides should be taken as far as possible into a single energy group; that is, the boundary points of the energy groups should not fall within the resonance peak.

### 2.2.1. 269-Group Structure

In order to test the influence of iron resonance on shielding calculations more accurately, this group structure was modified by the 199-group with 69 points interpolated into its group boundaries with an energy range from 1.1 keV to 3.1164 MeV. The interpolation was based on the characteristics of the resonances of the total cross section of Fe-56 in this energy range, as shown above. For example, there were three resolved resonance peaks between 79.5 and 82.5 keV. While the three peaks were contained in one group for the 199-group structure, they were subdivided into three groups for the 269-group structure, and each resonance peak belonged to one group separately. A comparison of these group divisions can be seen in Figure 2.

In order to test whether the 269-group structure is reasonable, it was necessary to compare it with other common energy group structures as introduced below.
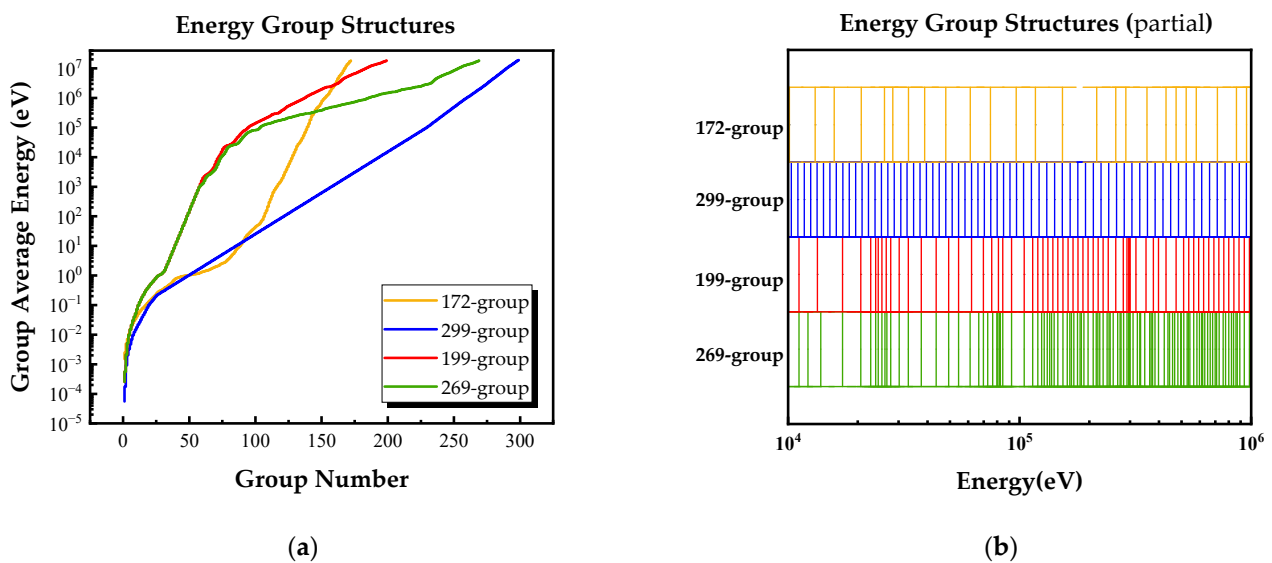
**Figure 2.** Four neutron group structures. (**a**) Comparison of four group structures in the entire energy range. (**b**) Comparison of four group structures between 10.0 keV and 1.0 MeV in which significant resonances occurred.

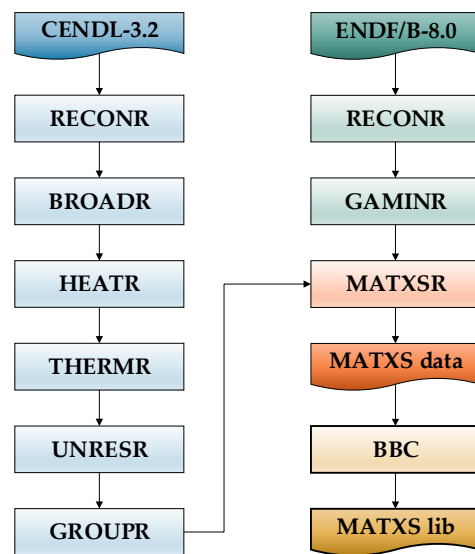2.2.2. Reference Multi-Group Structures

The bottom and upper energy limits of the 199-group structure are $10^{-5}$ eV and 19.64 MeV, respectively. There are 25 groups within the thermal energy range, which is below 1.0 eV. There are 78 groups in resonance range of Fe-56, which is from 10 keV to 2 MeV. The lethargy widths of each group are uniform, ranging from 0.025 to 0.25 above 1.0 eV.

The bottom and upper energy limits of the 299-group structure are $10^{-5}$ eV and 20 MeV, respectively. There are 48 groups within the thermal energy range, which is below 1.0 eV. There are 76 groups in resonance range of Fe-56, which is from 10 keV to 2 MeV. The lethargy widths of each group are uniform, ranging from 0.064 to 0.08 above 1.0 eV.

The bottom and upper energy limits of the 299-group structure are $10^{-5}$ eV and 19.64 MeV, respectively. There are 80 groups within the thermal energy range, which is below 1.0 eV. There are 30 groups in resonance range of Fe-56, which is from 10 keV to 2 MeV. The lethargy widths of each group are uniform, ranging from 0.01 to 0.4 above 1.0 eV.

Four different neutron energy group structures were employed. Only one gamma energy group structure (VITAMIN-B7 42 gamma group) was employed to match with these neutron groups. The gamma group structure was not tested in this study.

Four multi-group cross section libraries were generated by using NJOY [17] with the same inputs except for group structure. All the nuclides were processed at three temperature points (293.6 K, 600 K, and 900 K) with the standard weight function and free gas thermal scattering law. The Legendre expansion orders of the four libraries were all set to 8. The neutron-induced data were from the CENDL-3.2 evaluated nuclear data library and the photo-atomic data were from ENDF/B-8.0. As shown in Figure 3, the evaluated data were processed by the flow of RECORR, BROADR, HEATR, THERMR, UNRESR, GROUP, and GAMINR modules in NJOY and restored in MATXS format by MATXSR. The single MATXS files of each nuclide were then combined into one MATXS format multi-group library by BBC [16].

**Figure 3.** Processing flow of MATXS-format multi-group cross section library.

## 3. Selected SINBAD Benchmarks

In this study, 3 benchmarks of iron spherical shells with 12 different radii were selected for group structure analysis.

### 3.1. ill_fe

The iron sphere experiment was performed at the University of Illinois at Urbana-Champaign in 1975 [18]. This experiment calculated the neutron leakage on the surface of an iron sphere, and the calculated results were compared with the measured values to test the accuracy and effectiveness of the multi-group cross section libraries.

As shown in Figure 4, the 30.45 cm thick iron spherical shell had two cylindrical reentrant holes with plugs that provided access to the spherical central void. The flight tube of the neutron generator was inserted through the reentrant hole. The benchmark experiment was conducted using a DT fusion source, and its energy spectrum was calculated to be 14.08 MeV. The calculation model of the iron sphere had a radius of 38.10 cm and a wall thickness of 30.45 cm. The iron sphere contained 0.21% carbon, 0.47% manganese, 0.013% phosphorus, and 0.0024% sulfur.



(a)  (b)
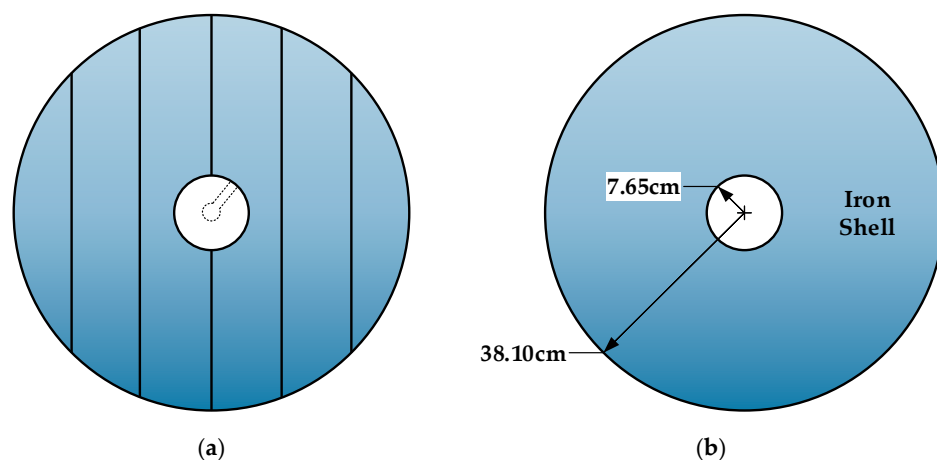
**Figure 4.** Geometry of ill_fe iron sphere benchmark. (**a**) Simplified geometry of experimental device. The solid line represents the surface of the assembled parts which are combined into a spherical device. The reentrant hole, which is used to place the DT neutron source, is represented by the dashed line in the central void region. (**b**) Simplified geometry used in one-dimensional $S_N$ calculation.
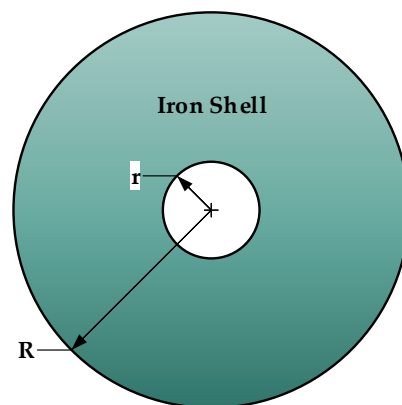
### 3.2. ippe_fe

This neutron transmission benchmark experiment was performed with 14 MeV neutrons through iron shells at the Institute of Physics and Power Engineering in the period from 1989 to 1995 [19]. This experiment calculated the neutron leakage on the surface of iron spheres with a 14 MeV D-T source in the center. The five spheres had radii from 4.5 to 30.0 cm and wall thicknesses from 2.5 to 28.0 cm, as shown in Figure 5. The calculated results were compared with the measured values to test the accuracy and effectiveness of the multi-group cross section libraries.



(**a**)                   (**b**)
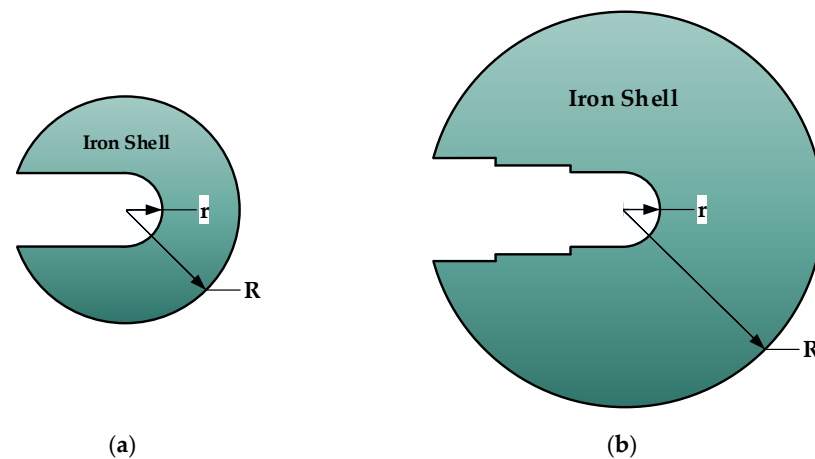
**Figure 5.** Geometry of ippe_fe iron sphere benchmark of shells and reentrant holes with various radii. (**a**) Simplified geometry of experimental device Shell 1, r = 2.0 cm, R = 4.5 cm. (**b**) Simplified geometry of experimental devices Shell 2 to 5, r = 4.5, 2.0, 1.9, and 2.0 cm, R = 12.0, 12.0, 20.0, and 30.0 cm, respectively.

Due to the background effects, the measured values should be corrected and converted to neutron leakage. The leakage was then normalized to one source neutron using a correction calculation. Thus, the thickness of each shell could simply be calculated from the value of R subtracted by r, and the iron sphere geometry could be simplified as shown in Figure 6. The iron spheres' nuclear densities were 8.385, 8.206, 8.210, 8.329, and 8.329 (atoms/(barn·cm)) for shells 1 to 5, respectively.



**Figure 6.** Simplified ippe_fe geometry of shells 1 to 5 used in one-dimensional S$_N$ calculation.

### 3.3. kfk_fe

The Karlsruhe iron sphere benchmark experiment was performed at the University of Illinois in 1975 [20]. This experiment calculated the neutron leakage on the surface of iron spheres with a Cf-252 source in the center. The six spheres had radii from 7.5 to 15.0 cm. The calculated results were compared with the measured values to test the accuracy and

effectiveness of the multi-group cross section libraries, especially for checking the iron inelastic scattering cross sections.

As shown in Figure 7, the center of the iron sphere is a cylindrical channel. A cylindrical container containing a Cf-252 source was inserted into the channel. In the simplified calculation model, the Cf-252 source was equivalent to a distributed spherical source.
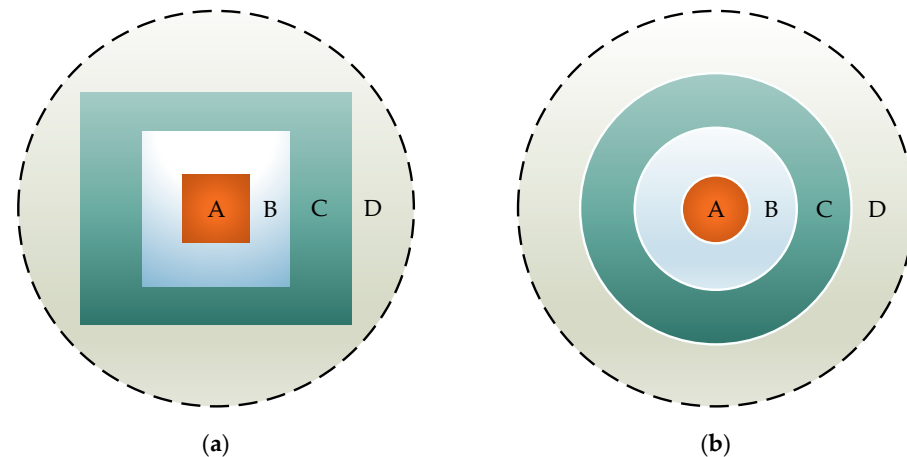


**Figure 7.** Geometry of source region of kfk_fe iron sphere benchmark. (**a**) Simplified geometry of experimental device. A, B, and C are the Cf-252 source, inner container, and outer container, respectively. D is the spherical iron shell. (**b**) Equivalent spherical source geometry based on volume ratio.

The measurements were integrated over the full sphere and normalized to one source neutron through a correction calculation. The square source areas in the benchmark were equivalent to spherical shells based on volume ratio, and six iron spheres with various radii were investigated. All the spheres had the same component materials (C 0.07%, Mn 0.05%, P 0.009%, and S 0.007%).

## 4. Results and Discussion

### 4.1. ill_fe

The calculated leakage spectra of the four multi-group libraries for the ill_fe iron sphere are compared with the experimental values in this work shown in Figure 8.
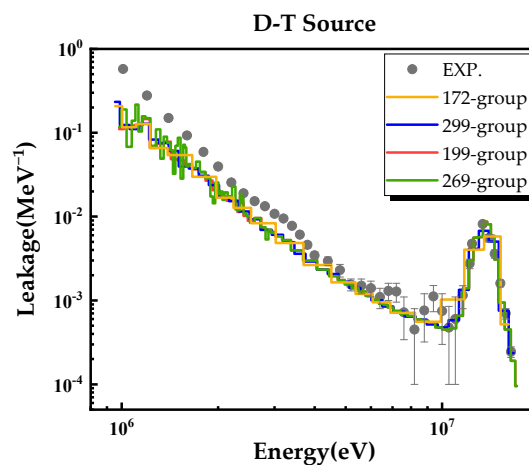


**Figure 8.** DT source neutron leakage spectra of iron sphere with outer radius 38.1 cm and thickness 30.45 cm.
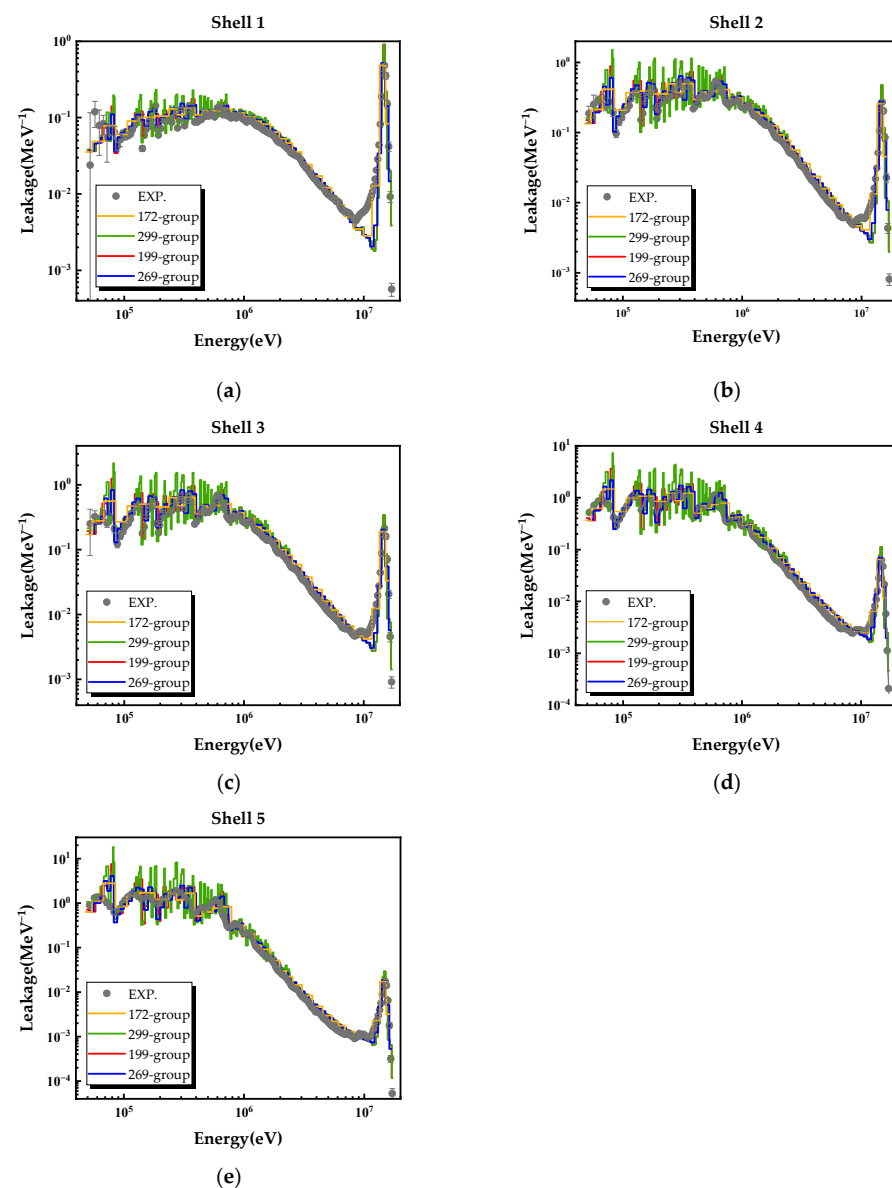
The four calculated leakages above 10.0 MeV were in good agreement with the measured values. Agreement between the four calculated leakages and the measured values

was relatively poor in the energy range of 5.0 to 10.0 MeV. All the calculated leakages disagreed less dramatically with the measurement values. The calculated results also underpredicted the spectra below 5.0 MeV.

Compared with the measured values in the energy range of 1.0 to 5.0 MeV, there were slight deficiencies in the calculated results. These were caused by a problem in representing the inelastic scattering cross sections. The MATXS format cross sections used in the ARES calculations were self-shielded for Fe-56. However, the self-shielding was applied to the elastic scattering and absorption cross sections. In this case, the inelastic scattering cross section in the vicinity of the threshold was too high. This problem produced the observed discrepancies between the ARES calculations and the measurement values.

### 4.2. ippe_fe

The calculated leakage spectra of the four multi-group libraries in this work for the ippe_fe iron spheres are compared with the experimental values in Figure 9.
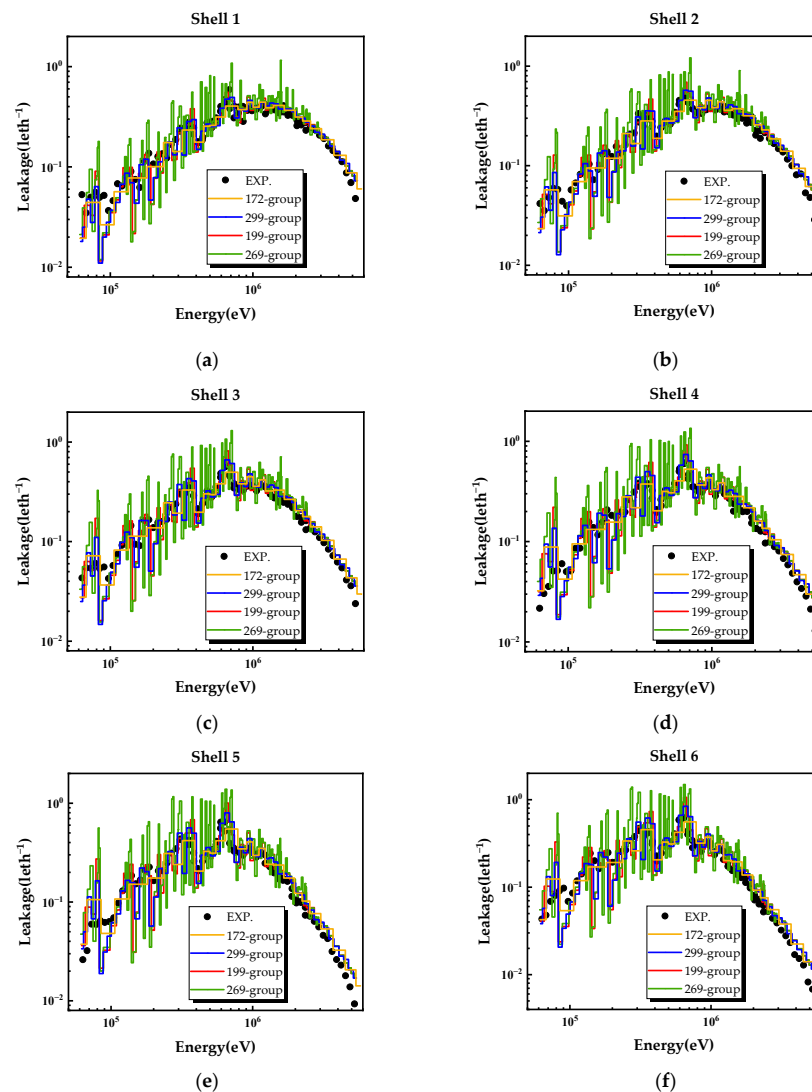


**Figure 9.** DT source neutron leakage spectra of iron spheres with five different outer radii and thicknesses. (**a**) Shell 1: radius 4.5 cm, thickness 2.5 cm. (**b**) Shell 2: radius 12 cm, thickness 7.5 cm. (**c**) Shell 3: radius 12 cm, thickness 10 cm. (**d**) Shell 4: radius 20 cm, thickness 18.1 cm. (**e**) Shell 5: radius 30 cm, thickness 28 cm.

The four calculated leakages were in good agreement with the measured values in the energy range of 0.75 to 8.2 MeV and above 13.1 MeV. In the energy range of 8.2 to 13.1 MeV, the calculated leakages of all four multi-group libraries deviated greatly from the measurements, which was due to inaccurate cross section data regarding the angular distribution of secondary neutrons in the evaluated nuclear data libraries. As the radii of the iron spheres increased, this deviation gradually decreased.

The calculated leakages of the 269-group library showed more obvious fluctuations than did the other multi-group libraries below 3.0 MeV because the 269-group structure had more boundaries in the energy range of 40 keV to 3.0 MeV than the others. There were 142 groups with a 269-group structure, while 76 had 199-group, 60 had 299-group, and 25 had 172-group structures in this energy region. The fluctuations were more significantly observed with the increase in the radii of the iron spheres. A larger number of energy groups could better represent the physical resonance phenomenon of the total cross section of Fe-56 in this energy range.

### 4.3. kfk_fe

The calculated leakage spectra of the four multi-group libraries in this work for the kfk_fe iron spheres are compared with the experimental values in Figure 10.



**Figure 10.** Cf-252 source neutron leakage spectra of iron spheres with six different thicknesses. (**a**) Shell 1: thickness 6.476 cm. (**b**) Shell 2: thickness 8.976 cm. (**c**) Shell 3: thickness 11.476 cm. (**d**) Shell 4: thickness 13.976 cm. (**e**) Shell 5: thickness 16.476 cm. (**f**) Shell 6: thickness 18.976 cm.

The neutron leakage spectra in the energy range between 1.0 and 3.0 MeV calculated with the four multi-group libraries were in good agreement with the measurements. However, as the radii of the iron spheres increased, the deviation between the calculated leakages and the measurements gradually increased above 3.0 MeV.

Compared with the measurements, the calculated leakages of the four multi-group libraries showed obvious fluctuations which increased as the radii of the iron spheres increased; however, they basically agreed with the spectral shape for resonances below 1.0 MeV. The leakage spectra of the 269-group showed more obvious fluctuations than the other group structures. This was the same for the benchmarks analyzed above.

### 4.4. Simple Fe-56 Test

The energy ranges of the three iron shielding benchmarks selected from SINBAD were all above 10.0 keV, so the calculation results of different energy group structures in the full energy range needed to be compared by setting simple test devices.

As shown in Figure 11, a 49.0 cm thick iron (Fe-56 only) spherical shell was obtained with four single energy sources (10.0, 1.0, 0.1, and 0.01 MeV) distributed in the central region with a 1.0 cm radius.
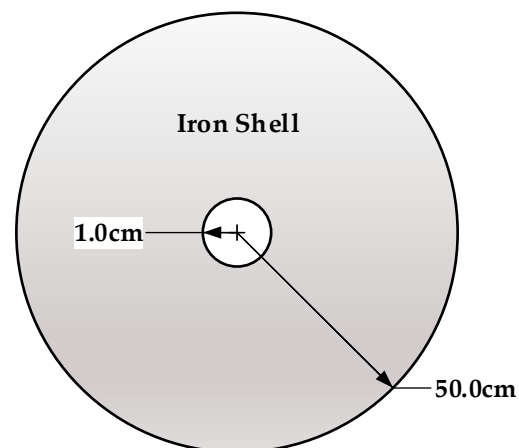


**Figure 11.** Simplified iron (Fe-56 only) shell geometry used in one-dimensional S$_N$ calculation.

The calculated leakage spectra of the four multi-group libraries for the iron sphere with different sources are compared with each other in Figure 12.

It can be inferred from these results that the 172-group structure was in significant disagreement with the other three group structures below 20 keV because it had only one group between 16.6 and 24.8 keV, whereas the other group structures had at least five groups to represent the very large resonance peaks in the energy range. That is to say, the 172-group structure was not suitable for iron shielding calculation but was more suitable for core physics calculation due to its far higher number of groups in the thermal energy range.

The results of the 269-group, 199-group, and 299-group structures were in good agreement with each other at 10.0, 1.0, and 0.01 MeV. The result of the 199-group structure at 0.1 MeV showed some deviation from the other results. This indicates that the 199-group structure still has problems that require improvement under specific neutron source conditions in the future.
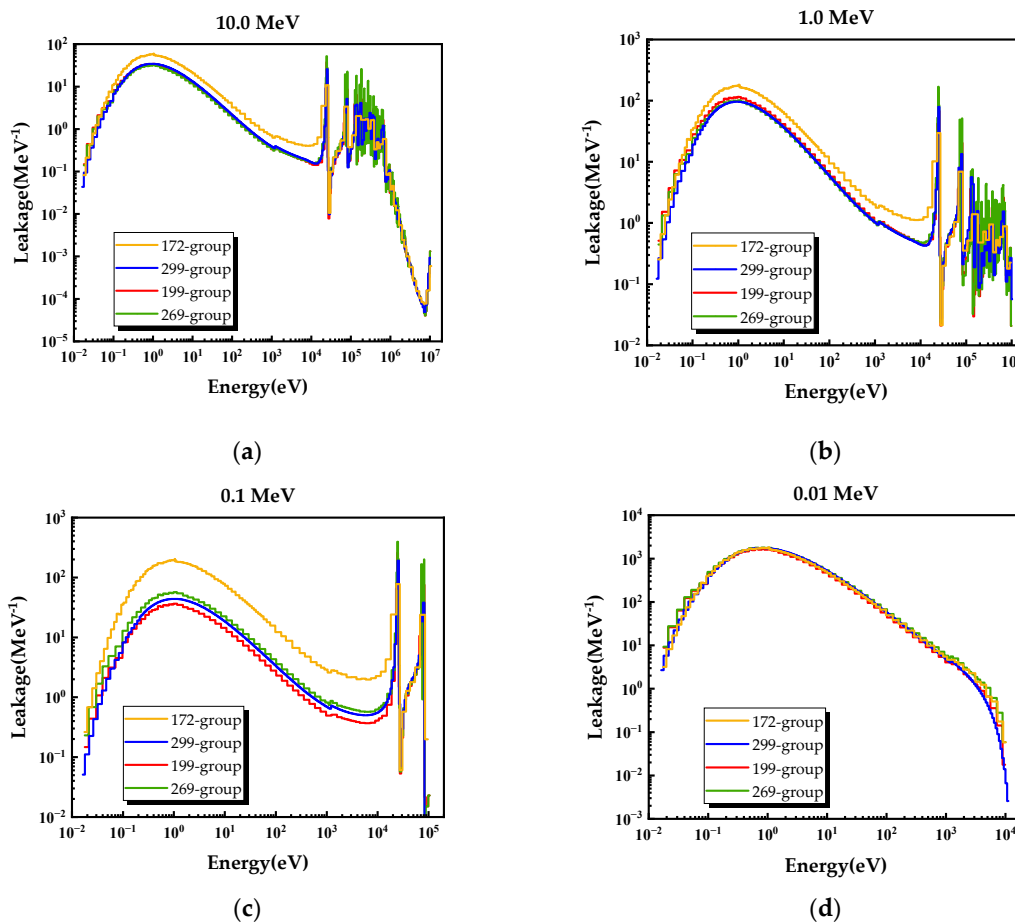
**Figure 12.** Four different single-energy source neutron leakage spectra for iron spheres: (**a**) 10.0 MeV, (**b**) 1.0 MeV, (**c**) 0.1 MeV, and (**d**) 0.01 MeV.

## 5. Conclusions

In this study, 3 benchmarks of iron spherical shells with 12 different radii were selected for neutron group structure analysis, which was performed using the discrete ordinate method code ARES with multi-group libraries. A 269-neutron-group library was generated by using NJOY code due to the resonance of the total cross section of Fe-56 based on CENDL-3.2, and three other multi-group libraries (199-group, 299-group, and 172-group) were also generated with the same parameters. With respect to the analyses, the resonance of Fe-56 had a great influence on the accuracy of the calculated leakage. Further, it is noted that the finer the energy group division, the greater the calculated leakage fluctuation, and the deeper the neutron passed through the iron sphere, the larger the calculated leakage fluctuation. The widely used energy group structures still require further analysis and improvement to meet the higher accuracy requirements for iron shielding calculation.

The deviation of calculated leakages of different multi-group structures may impact certain neutron shielding designs. Consequently, neutron shielding designers should consider the differences between various multi-group structures, paying particular attention to the resonance characteristics of important shielding materials. This study and its leakage results may provide a good reference for the development of new multi-group structures for present and future shielding design.

## References

1.  Lathrop, K.D. *DTF-IV, a Fortran-IV Program for Solving the Multigroup Transport Equation with Anisotropic Scattering*; LA-3373; Los Alamos Scientific Laboratory of the University of California: Los Alamos, NM, USA, 1965.
2.  Hansen, G.E.; Roach, W.H. *Six and Sixteen Group Cross Sections for Fast and Intermediate Critical Assemblies*; LAMS-2543; Los Alamos National Laboratory: Los Alamos, NM, USA, 1961.
3.  Bandarenko, I.I.; Abagyan, L.P. *Group Constants for Nuclear Reactor Calculations*; Consultanta Buren: New York, NY, USA, 1964.
4.  Santamarina, A.; Hfaiedh, N.; Letellier, R.; Marotte, V.; Misu, S.; Sargeni, A.; Vaglio, C. Zmijarevic. Advanced neutronics tools for BWR design calculations. *Nucl. Eng. Des.* **2008**, *238*, 1965–1974. [CrossRef]
5.  Hykes, J.M.; Ferrer, R.M. Validation of CASMO5 neutron kinetics parameters. *Ann. Nucl. Energy* **2020**, *136*, 107015. [CrossRef]
6.  Deen, J.R.; Woodruff, W.L.; Costescu, C.I. *WIMS-D4M User Manual (Rev. 0)*; ANL/RERTR/TM-23; Argonne National Laboratory: Argonne, IL, USA, 1995.
7.  Roussin, R.W. *BUGLE-80: A Coupled 47-Neutron, 20-Gamma-Ray Group Library for LWR Shielding Calculations*; Oak Ridge National Laboratory: Oak Ridge, TN, USA, 1980.
8.  Risner, J.M.; Wiarda, D.; Dunn, M.E.; Miller, T.M.; Peplow, D.E.; Patton, B.W. *Production and Testing of the VITAMIN-B7 Fine-Group and BUGLE-B7 Broad-Group Coupled Neutron/Gamma Cross Section Libraries Derived from ENDF/B-VII.0 Nuclear Data*; NUREG/CR-7045, ORNL/TM-2011/12; Oak Ridge National Laboratory: Oak Ridge, TN, USA, 2011.
9.  Alpan, F.A.; Haghighat, A. Development of the CPXSD Methodology for Generation of Fine-Group Libraries for Shielding Applications. *Nucl. Sci. Eng. J. Am. Nucl. Soc.* **2005**, *149*, 51–64. [CrossRef]
10. Iwamoto, O.; Iwamoto, N.; Kunieda, S.; Minato, F.; Nakayama, S.; Abe, Y.; Tsubakihara, K.; Okumura, S.; Ishizuka, C.; Yoshida, T.; et al. Japanese Evaluated Nuclear Data Library version 5: JENDL-5. *Nucl. Sci. Technol.* **2023**, *60*, 1–60. [CrossRef]
11. Brown, D.A.; Chadwick, M.B.; Capote, R.; Kahler, A.C.; Trkov, A.; Herman, M.W.; Sonzogni, A.A.; Danon, Y.; Carlson, A.D.; Dunn, M.; et al. ENDF/B-VIII.0: The 8th Major Release of the Nuclear Reaction Data Library with CIELO-project Cross Sections, New Standards and Thermal Scattering Data. *Nucl. Data Sheets* **2018**, *148*, 1–142. [CrossRef]
12. Ge, Z.; Xu, R.; Wu, H.; Zhang, Y.; Chen, G.; Jin, Y.; Shu, N.; Chen, Y.; Tao, X.; Tian, Y.; et al. CENDL-3.2: The New Version of Chinese General Purpose Evaluated Nuclear Data Library. *EPJ Web Conf.* **2020**, *239*, 09001. [CrossRef]
13. Kodeli, I.; Sartori, E.; Kirk, B. SINBAD Shielding Benchmark Experiments Status and Planned Activities. In Proceedings of the American Nuclear Society's 14th Biennial Topical Meeting of the Radiation Protection and Shielding Division, Carlsbad, NM, USA, 3–6 April 2006.
14. Chen, Y.; Zhang, B.; Zhang, L.; Zheng, J.; Zheng, Y.; Liu, C. ARES: A parallel discrete ordinates transport code for radiation shielding applications and reactor physics analysis. *Sci. Technol. Nucl. Ins.* **2017**, *2017*, 2596727. [CrossRef]
15. Engle, W.W., Jr. *A Users Manual for ANISN: A One-Dimensional Discrete Ordinates Transport Code with Anisotropic Scattering*; K-1693 Report; Oak Ridge National Laboratory: Oak Ridge, TN, USA, 1973.
16. MacFarlane, R.E. *TRANSX 2: A Code for Interfacing MATXS Cross Section Libraries to Nuclear Transport Codes*; LA-12312-MS; Los Alamos National Laboratory: Los Alamos, NM, USA, 1992.
17. Macfarlane, R.E. NJOY 99/2001: New Capabilities in Data Processing. In Proceedings of the American Nuclear Society 12th Biennial RPSD Topical Meeting, Santa Fe, NM, USA, 14–18 April 2002; Department of Energy of United States: Washington, DC, USA, 2002.
18. Williams, M.L.; Aboughantous, C.; Asgari, M.; White, J.E.; Wright, R.Q.; Kam, F.B.K. Transport Calculations of Neutron Transmission Through Steel Using ENDF/B-V, Revised ENDF/B-V, and ENDF/B-VI Iron Evaluations. *Annu. Nucl. Energy* **1991**, *18*, 549–565. [CrossRef]
19. Simakov, S.P.; Devkin, B.V.; Kobozev, M.G.; Talalaev, V.A.; Fischer, U.; von Möllendorff, U. *Validation of Evaluated Data Libraries Against an Iron Shell Transmission Experiment and Against the Fe(n,xn) Reaction Cross Section with 14 MeV Neutron Source*; EFF-DOC-747; NEA Data Bank: Paris, France, 2000.
20. Werle, H.; Bluhm, H.; Fieg, G.; Kappler, F.; Kuhn, D.; Lalovic, M. Neutron Leakage Spectra from Iron Spheres with a Cf-252 Neutron Source in the Centre. In Proceedings of the Specialists' Meeting on Sensitivity Studies and Shielding Benchmarks, Paris, France, 7 October 1975.